Available online at www.sciencedirect.com
ScienceDirect
Journal of Computational Physics 219 (2006) 498–512
JOURNAL OF COMPUTATIONAL PHYSICS
www.elsevier.com/locate/jcp

Review

Dynamic analysis of fluid–soil–structure interaction problems by the boundary element method

D. Soares Jr. [a,b,*], W.J. Mansur [a]

[a] Department of Civil Engineering, COPPE – Federal University of Rio de Janeiro, CP 68506, CEP 21945-970, Rio de Janeiro, RJ, Brazil
[b] Structural Engineering Department, Federal University of Juiz de Fora, Cidade Universitária, CEP 36036-330, Juiz de Fora, MG, Brazil

Received 7 September 2005; received in revised form 19 April 2006; accepted 20 April 2006
Available online 19 June 2006

Abstract

The present paper describes an iterative procedure for BEM–BEM coupling. The paper presents suitable interface conditions and algorithms for iteratively coupling sub-domains modeled by three different boundary element time-domain formulations, namely: acoustic and elastodynamic BEM formulations based on time-dependent Green's functions and non-linear time-domain approach which employs elastostatic Green's functions and therefore requires domain discretization. Two examples are analyzed and at the end of the paper conclusions of the study are presented.

Keywords: Time-domain BEM; Iterative BEM–BEM coupling; Acoustics; Elastodynamics; Plasticity

1. Introduction

Numerical solution algorithms for wave propagation analysis may give inaccurate results or else become unstable when the medium being considered is composed of sub-domains with too different physical properties, when different media interact either through common interfaces, as is the case of soil–fluid–structure interaction analyses, or by forming a mixture, e.g. poroelastic media. Inaccurate and unstable time-domain algorithms may also occur when two different numerical methods are coupled, e.g. the boundary element method (BEM) and the finite element method (FEM); this problem may become even more serious when coupled algorithms and different physical media are considered simultaneously in the same analysis.

There are many strategies in the FEM literature concerning the subject described in the last paragraph [1,2], one simple but efficient approach being subcycling [3–5]. Researchers dealing with the finite difference method (FDM) also proposed strategies to deal with interaction between different media; robust strategies have been proposed, some of them are widely used [6–8]. When no special procedure is employed to deal with this problem, e.g. assemble of the global matrix follows standard FEM procedures for homogeneous media, the

* Corresponding author.
E-mail addresses: delfim@coc.ufrj.br (D. Soares Jr.), webe@coc.ufrj.br (W.J. Mansur).

0021-9991/$ - see front matter
doi:10.1016/j.jcp.2006.04.006

coupling between two different regions is referred to as ''direct coupling''; subcycling and other iterative strategies will be referred here as ''iterative coupling''.

The idea of direct coupling BEM sub-domains by enforcing equilibrium and compatibility of common interface unknowns are reported in the very first BEM texts [9]. The direct coupling idea was soon extended to couple the BEM with other numerical methods, especially the FEM, as reported by Zienkiewicz et al. [10] and Brebbia and Georgiou [11], for static problems. Less than a decade afterwards, direct coupling procedures started being employed to many problems, including time-domain wave propagation modeling.

Many algorithms have already been reported concerning BEM–FEM direct coupling for time-domain wave propagation (acoustic, elastic, etc.) analysis [12–18]. On those algorithms, boundary elements either played the rule of a transmitting boundary or (less usual) modeled parts of the domain most suitable to BEM modeling. A good transmitting boundary is in fact a critical requirement in wave propagation analyses of infinite domain problems, because when waves are not properly transmitted to infinity, artificial reflections on the transmitting boundaries may very soon invalidate results.

Most papers dealing with time-domain fluid–soil–structure interaction employ direct coupling to fulfill equilibrium and compatibility conditions on BEM–BEM or BEM–FEM interfaces. Initial papers dealing with BEM–FEM/BEM–BEM coupling for fluid–structure (acoustic–elastic may be a more adequate designation) interaction were concerned with the establishment of a suitable direct coupling approach [14], which could be extended to more complex cases, e.g. non-linear models [18]. More recently, publications concerning stability started appearing, enabling the classical direct coupling algorithms to be applied to more severe situations [19,20]. Direct coupling for soil–structure interaction has also been exhaustively studied, following guidelines similar to those concerning fluid–structure interaction [12,13,15,17].

In recent years, iterative coupling algorithms have been reported as a promising technique [21]: they may become more accurate, stable, flexible and cheaper than direct coupling procedures. In the iterative coupling algorithms, equilibrium and compatibility at common interfaces are achieved iteratively. The cost of each iteration is much lower than that of direct coupling algorithms, as the order of the various system of equations to be solved in each iteration is typically lower than the order of the system obtained with direct coupling approaches. Thus, as usually the algorithm converges in very few iterations and the iterative process is already necessary in order to solve some possible non-linear behavior, the overall cost of the iterative coupling is lower than that of the direct coupling. Moreover, as each sub-domain is solved independently, one may take advantage of the characteristics of each system of equations, in order to reduce the computer time. This possibility can be explored when different numerical methods are employed (e.g. FEM matrices are symmetric, positive definite and sparse, whereas BEM matrices are non-symmetric and fully populated) or else, when different media are present and iterative solvers are employed for each sub-domain.

The good performance reported in the literature by iterative coupling for time-independent problems [22,23] encouraged researchers to work out procedures for time-dependent problems. Only a few papers concerning this subject have been published so far, most of them dedicated to BEM–FEM coupling [24–26]. For a detailed text concerning iterative BEM–BEM coupling in time domain, the reader is referred to Soares Jr. et al. [27]. As reported by Soares Jr. et al. [24–27], besides being cheaper than direct coupling algorithms, iterative coupling approaches are quite robust, and should be preferred especially in the case where there are media with quite different physical properties (of the same or different nature). As it has been shown [26], iterative coupling algorithms are stable in cases where direct coupling procedures are not, as the former easily allows considering different time-steps for different sub-domains.

In a previous paper [27], the authors reported good results for a time-domain iterative BEM–BEM coupling approach, being the classical TD-BEM formulation [28] employed to model infinite sub-regions and the D-BEM approach [29] employed to model regions having plastic behavior. This approach is briefly reviewed here, for the sake of completeness. The present paper describes the conditions for iteratively coupling sub-domains modeled by three different boundary element time-domain formulations: (i) formulation I: the acoustic time-domain formulation presented by Mansur [28], which is based on time-dependent Green's functions; (ii) formulation II: the elastodynamic time-domain formulation presented by Mansur [28], also based on time-dependent Green's functions; (iii) formulation III: the elastodynamic time-domain approach which employs the static case Green's functions, and therefore requires domain discretization. This last formulation is used here to model regions with plastic behavior.

Two examples are presented, results being compared with those obtained by direct coupling approaches. At the end of the paper, the conclusions of the study are presented.

2. Boundary element formulations

The first BE formulation focused here is for acoustics and in Section 2.1, the basic BE equations for the solution of acoustic fluids are shown. In the sequence (Sections 2.2 and 2.3), two BE formulations related to dynamic problems are presented: the first one considers dynamic time-domain fundamental solutions and the second one makes use of static fundamental solutions. In the present work, soils or/and structures will be modeled by these dynamic BE formulations. Once the selected boundary element formulations have been briefly discussed, the coupling of these different techniques is considered in Section 3.

2.1. Formulation I

In the present section, acoustic wave propagation in fluids is considered. The integral equation, which solves the acoustic model in focus, is given by [28]:

$$c(\xi)p(\xi,t) = \int_0^{t+} \int_\Gamma p^*(X,t;\xi,\tau)q(X,\tau)\,\mathrm{d}\Gamma(X)\,\mathrm{d}\tau - \int_0^{t+} \int_\Gamma q^*(X,t;\xi,\tau)p(X,\tau)\,\mathrm{d}\Gamma(X)\,\mathrm{d}\tau + s(X,t;\xi,\tau) \tag{1}$$

where Γ is the boundary of the body, $c(\xi)$ depends on the geometry and the terms $p^*(X,t;\xi,\tau)$ and $q^*(X,t;\xi,\tau)$ represent the fundamental potential (hydrodynamic pressure) and flux, respectively. X is the field point; ξ is the source point and $s(X,t;\xi,\tau)$ stands for possible domain integrals contributions (initial conditions or/and body forces).

Adopting the following space-time approximations for the variables of the model (η and ϕ are space and time interpolation functions, respectively, related to a boundary node j and a discrete time m):

$$p(X,t) = \sum_{j=1}^{J}\sum_{m=1}^{M} \phi_p^m(t)\eta_p^j(X)p_j^m \tag{2a}$$

$$q(X,t) = \sum_{j=1}^{J}\sum_{m=1}^{M} \phi_q^m(t)\eta_q^j(X)q_j^m \tag{2b}$$

the following system of equations can be obtained:

$$\mathbf{C}\mathbf{P}^n = \mathbf{G}^1\mathbf{Q}^n - \mathbf{H}^1\mathbf{P}^n + \mathbf{L}^n + \mathbf{S}^n \tag{3a}$$

$$\mathbf{L}^n = \sum_{m=1}^{n-1}(\mathbf{G}^{n-m+1}\mathbf{Q}^m - \mathbf{H}^{n-m+1}\mathbf{P}^m) \tag{3b}$$

where $\mathbf{C}$, $\mathbf{G}$ and $\mathbf{H}$ are influence matrices; $\mathbf{L}^n$ is a vector standing for the time convolution process; $\mathbf{S}^n$ is a vector related to domain integrals and $\mathbf{P}^n$ and $\mathbf{Q}^n$ are pressure and flux vectors, respectively, at the discrete time n. After introducing the boundary conditions of the model, the system of equations (3) can be solved for pressures and fluxes, at each time t_n. For more details concerning the present formulation, the reader is referred to [21,28,30].

2.2. Formulation II

In the present section, dynamic linear models are considered. The integral equation based on dynamic fundamental solutions that solves the model in focus is given by [28]:

$$c_{ik}(\xi)u_k(\xi,t) = \int_0^{t+} \int_\Gamma u_{ik}^*(X,t;\xi,\tau)\tau_k(X,\tau)\,\mathrm{d}\Gamma(X)\,\mathrm{d}\tau - \int_0^{t+} \int_\Gamma \tau_{ik}^*(X,t;\xi,\tau)u_k(X,\tau)\,\mathrm{d}\Gamma(X)\,\mathrm{d}\tau + s(X,t;\xi,\tau) \tag{4}$$

where the terms $u^*_{ik}(X,t;\xi,\tau)$ and $\tau^*_{ik}(X,t;\xi,\tau)$ represent the dynamic fundamental displacement and traction, respectively (the remainder terms and symbols of Eq. (4) are analogous to the ones depicted in Eq. (1)). Adopting the following space-time approximations for the variables of the model:

$$u_k(X,t) = \sum_{j=1}^{J}\sum_{m=1}^{M} \phi_u^m(t)\eta_u^j(X)u_{kj}^m \tag{5a}$$

$$\tau_k(X,t) = \sum_{j=1}^{J}\sum_{m=1}^{M} \phi_\tau^m(t)\eta_\tau^j(X)\tau_{kj}^m \tag{5b}$$

the following system of equations can be obtained:

$$\mathbf{C}\mathbf{U}^n = \mathbf{G}^1\mathbf{T}^n - \mathbf{H}^1\mathbf{U}^n + \mathbf{L}^n + \mathbf{S}^n \tag{6a}$$

$$\mathbf{L}^n = \sum_{m=1}^{n-1}(\mathbf{G}^{n-m+1}\mathbf{T}^m - \mathbf{H}^{n-m+1}\mathbf{U}^m) \tag{6b}$$

where the definition of $\mathbf{C}$, $\mathbf{G}$, $\mathbf{H}$, $\mathbf{L}^n$ and $\mathbf{S}^n$ is analogous to that of Section 2.1 and $\mathbf{U}^n$ and $\mathbf{T}^n$ are displacement and traction vectors, respectively, at the discrete time n. After introducing the boundary conditions of the model, the system of equations (6) can be solved for displacements and tractions, at each time t_n. For more details concerning the present formulation, the reader is referred to [21,27,28,30]. The BE formulations I and II are meant to be employed here mainly as a "transmitting boundary", thus, initial conditions and source density contributions have not been considered. The reader is referred to Refs. [28,31] for a thorough discussion on this topic.

2.3. Formulation III

In the present section, dynamic non-linear models are considered. The integral equations based on static fundamental solutions that solves the model in focus (displacements and stresses) are given by [32]:

$$c_{ik}(\xi)u_k(\xi,t) = \int_\Gamma u^*_{ik}(X;\xi)\tau_k(X,t)\,\mathrm{d}\Gamma(X) - \int_\Gamma \tau^*_{ik}(X;\xi)u_k(X,t)\,\mathrm{d}\Gamma(X) + \int_\Omega \varepsilon^*_{ikj}(X;\xi)\sigma^P_{kj}(X,t)\,\mathrm{d}\Omega(X) - \int_\Omega u^*_{ik}(X;\xi)\rho\{\ddot{u}_k(X,t) - b_k(X,t)\}\,\mathrm{d}\Omega(X) \tag{7}$$

$$\sigma_{ik}(\xi,t) = \int_\Gamma u^*_{ikj}(X;\xi)\tau_j(X,t)\,\mathrm{d}\Gamma(X) - \int_\Gamma \tau^*_{ikj}(X;\xi)u_j(X,t)\,\mathrm{d}\Gamma(X) + g_{ik}(X,t) + \int_\Omega \varepsilon^*_{ikjl}(X;\xi)\sigma^P_{jl}(X,t)\,\mathrm{d}\Omega(X) - \int_\Omega u^*_{ikj}(X;\xi)\rho\{\ddot{u}_j(X,t) - b_j(X,t)\}\,\mathrm{d}\Omega(X) \tag{8}$$

where Ω is the domain of the body and the terms $u^*_{ik}(X;\xi)$, $\tau^*_{ik}(X;\xi)$ and $\varepsilon^*_{ikj}(X;\xi)$, as well as $u^*_{ikj}(X;\xi)$, $\tau^*_{ikj}(X;\xi)$ and $\varepsilon^*_{ikjl}(X;\xi)$, represent the elastostatic fundamental solutions. $b_j(X,t)$ stands for body forces terms; ρ is the mass density of the model and $\ddot{u}_j(X,t)$ stands for the accelerations of the problem to be solved. $\sigma^P_{jl}(X,t)$ represents the "initial" (plastic) stress components and the free term $g_{ik}(\sigma^P_{jl}(X,t))$ is due to the derivative of the initial stress domain integral [33].

Adopting the following generic space approximation for the variables of the model (j stands for boundary element nodes or cell nodes; dual reciprocity formulations are also possible):

$$v_k(X,t) = \sum_{j=1}^{J} \eta_v^j(X)v_{kj}(t) \tag{9}$$

the following system of equations can be obtained, after suitable algebraic operations:

$$\mathbf{C}\mathbf{U}^n = \mathbf{G}\mathbf{T}^n - \mathbf{H}\mathbf{U}^n + \mathbf{W}\mathbf{O}^n_p - \mathbf{M}\ddot{\mathbf{U}}^n + \mathbf{S}^n \tag{10}$$

$$\mathbf{O}^n = \mathbf{G}'\mathbf{T}^n - \mathbf{H}'\mathbf{U}^n + \mathbf{W}'\mathbf{O}^n_p - \mathbf{M}'\ddot{\mathbf{U}}^n + \mathbf{S}'^n \tag{11}$$

where matrices **H**, **G**, **H**′ and **G**′ correspond to the boundary integrals while matrices **M**, **W**, **M**′ and **W**′ correspond to the inertial and initial stress domain integrals (the free term depicted in Eq. (8) is dealt with in **W**′). Vector $\mathbf{O}^n$ stands for the stress nodal values. $\mathbf{S}^n$ and $\mathbf{S}'^n$ are the vectors related to body force terms and $\mathbf{U}^n$ and $\mathbf{T}^n$ are displacement and traction vectors, respectively, at time step n.

To solve the system of equations (10) and (11) the boundary conditions of the model have to be considered and a time-integration scheme has to be adopted (the present work adopts the Houlbot method [34]). Moreover, an iterative algorithm must be considered in order to properly evaluate the problem stress state (elasto-plastic model). The present work adopts the Newton–Raphson scheme in order to deal with non-linear effects [35].

After considering the above-mentioned procedures, the system of equations (10) and (11) can be solved for displacements, tractions and stresses, at each time step. For more details concerning the present formulation, the reader is referred to [21,27,29,32,35].

3. Coupling procedures

In the present section, a discussion concerning the iterative coupling of the BE formulations previously presented is carried out. As it has been shown [24–27], iterative coupling is a very versatile procedure. It allows independent modeling of each sub-domain of the global model: interaction effects are considered by boundary values, which are iteratively updated along the common interfaces.

In the present text, firstly (Section 3.1) some special procedures, which are used in conjunction with the adopted iterative coupling, are discussed. In the sequence, the coupling of BE formulations I and III is described, followed by the coupling of BE formulations I and II. The coupling of BE formulations II and III was discussed in detail in a previous work of the authors [27], thus, just some basic aspects of this coupling procedure are presented here.

3.1. Special procedures

The present section describes some important procedures with which the coupled numerical solution becomes more efficient, accurate and stable. These special procedures are, namely: (i) adoption of a relaxation parameter α in order to ensure or/and speed up the convergence of the iterative coupling process; (ii) adoption of space/time interpolation/extrapolation procedures in order to consider independent discretizations for the different BE formulations.

In the iterative coupling procedures, a relaxation parameter α is introduced, which relates the recent BEM results ($^{(k+\alpha)}\mathbf{V}$) with the results of the previous iterative step ($^{(k)}\mathbf{V}$) and the final results ($^{(k+1)}\mathbf{V}$) at the current iterative step. Considering a generic variable **V**, the adoption of the relaxation parameter α can be described as follows:

$$^{(k+1)}\mathbf{V} = (\alpha)^{(k+\alpha)}\mathbf{V} + (1-\alpha)^{(k)}\mathbf{V} \tag{12}$$

In order to consider different time-steps in each sub-domain, interpolation/extrapolation procedures along time may be considered. In the present work, the interpolation/extrapolation procedures are based on the BEM time interpolation functions (e.g. piecewise constant $\phi_q(t)$ and linear $\phi_p(t)$ – Eq. (2)), as depicted by

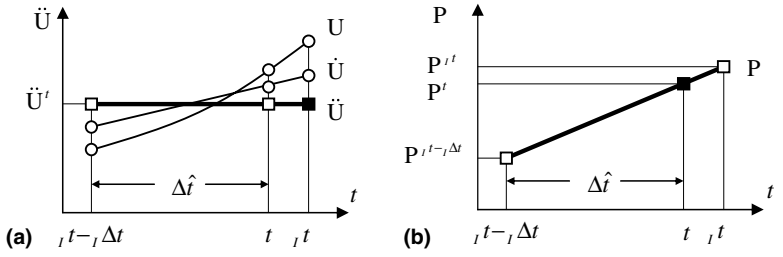

Fig. 1. Time interpolation/extrapolation procedures: (a) time extrapolation, $\ddot{\mathrm{U}}^{t} = \ddot{\mathrm{U}}^{t}$; (b) time interpolation, $P^{t} = P^{t}(\Delta\hat{t}/{}_1\Delta t) + P^{t-{}_1\Delta t}(1 - \Delta\hat{t}/{}_1\Delta t)$.

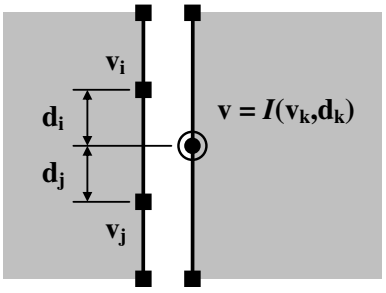

Fig. 2. Space interpolation procedures: interpolation scheme of $\mathbf{v}_k$ values in order to obtain $\mathbf{v}$ (linear interpolation: $\mathbf{v} = (\mathbf{v}_i\mathbf{d}_j + \mathbf{v}_j\mathbf{d}_i)/(\mathbf{d}_j + \mathbf{d}_i)$).

Fig. 1. This figure describes the calculus of some variables that are necessary for the algorithms presented in the following sections (in the present discussion, it is considered that the solid sub-domain time-step is smaller than the fluid sub-domain time-step, which is usual). Space interpolation procedures may also be adopted in order to consider independent BE meshes. In Fig. 2, for instance, a simple scheme is shown to evaluate nodal values of a sub-domain by means of the nodal values of the adjacent sub-domain, when there is not a direct connection among the nodes. Using space/time interpolation/extrapolation procedures, optimal modeling of each sub-domain may be achieved, which is very important in what concerns flexibility, efficiency, accuracy and stability aspects.

3.2. Coupling of formulations I and III

For a fluid–solid interaction problem, the boundary conditions at coupling interfaces, taking into account BE formulations I and III, are given by:

$$ {}_{\mathrm{III}}\mathbf{T}^t_{\mathrm{T}} = \mathbf{0} \tag{13a}$$

$$ {}_{\mathrm{III}}\mathbf{T}^t_{\mathrm{N}} + {}_{\mathrm{I}}\mathbf{P}^t = \mathbf{0} \tag{13b}$$

$$ {}_{\mathrm{III}}\ddot{\mathbf{U}}^t_{\mathrm{N}} - {}_{\mathrm{I}}\ddot{\mathbf{U}}^t = \mathbf{0} \tag{13c}$$

where Eq. (13) is written based on the coupling of BE formulations I and III for a given time value t (thus the left-side subscripts I and III and the right-side superscript t). The right-side subscripts N and T stand for the interface normal and tangential components, respectively. In Eq. (13c), the equivalent acceleration ${}_{\mathrm{I}}\ddot{\mathbf{U}}^t$ is given by ${}_{\mathrm{I}}\ddot{\mathbf{U}}^t = (1/\rho){}_{\mathrm{I}}\mathbf{Q}^t$, where ρ is the mass density of the fluid.

In the iterative coupling approach being considered, natural boundary conditions are prescribed, at the common interfaces, for each sub-domain (either modeled by the BE formulation I or III). The accelerations evaluated at the sub-domains modeled by formulation III are used to obtain the fluxes (prescribed interface boundary condition) for the sub-domains modeled by formulation I (Eq. (13c)); the pressures evaluated at the sub-domains modeled by formulation I are used to obtain the tractions (prescribed interface boundary condition) for the sub-domains modeled by formulation III (Eqs. (13a) and (13b)). Concisely, each sub-domain is solved separately (${}_{\mathrm{III}}\ddot{\mathbf{U}}^t$ and ${}_{\mathrm{I}}\mathbf{P}^t$ are evaluated at each iterative step) and the interface relations ${}_{\mathrm{III}}\ddot{\mathbf{U}}^t \rightarrow {}_{\mathrm{I}}\mathbf{Q}^t$ and ${}_{\mathrm{I}}\mathbf{P}^t \rightarrow {}_{\mathrm{III}}\mathbf{T}^t$ are iteratively considered until convergence is achieved. A basic algorithm solution for the coupling of BE formulations I and III is shown in Table 1.

3.3. Coupling of formulations I and II

For the coupling of formulations I and II, Eq. (13) can analogously be used; however, since BE formulation II usually does not evaluate accelerations, Eq. (13c) must be adapted.

In order to relate the fluxes (${}_{\mathrm{I}}\mathbf{Q}^t$) of the BE formulation I with the displacements (${}_{\mathrm{II}}\mathbf{U}^t$) of the BE formulation II (adaptation of relation (13c)), the characteristics of the time interpolation function $\phi_q(t)$ is here taken into account. Once the present work adopts $\phi_q(t)$ as being piecewise constant, an equivalent displacement ${}_{\mathrm{I}}\mathbf{U}^t$ can be obtained from the equivalent acceleration ${}_{\mathrm{I}}\ddot{\mathbf{U}}^t$ by time integration, as follows:

Table 1
Iterative coupling of BE formulations I and III

(1) Initial calculations
  (1.1) Time steps for each sub-domain are selected (${}_{\mathrm{I}}\Delta t, {}_{\mathrm{III}}\Delta t$)
    The following initial time attribution is adopted: ${}_{\mathrm{I}}t = {}_{\mathrm{I}}\Delta t$; ${}_{\mathrm{III}}t = 0$
  (1.2) BEM standard initial calculations are considered (e.g. influence matrices $\mathbf{G}^1$, $\mathbf{H}^1$, etc.)
  (1.3) Initial prescribed values are chosen at the common interface surfaces (e.g. ${}^{(0)}_{\mathrm{III}}\mathbf{T} = \mathbf{0}$)

(2) Time-step loop
  (2.1) Beginning of evaluations at each time step:
    update ${}_{\mathrm{III}}t = {}_{\mathrm{III}}t + {}_{\mathrm{III}}\Delta t$
    If ${}_{\mathrm{III}}t > {}_{\mathrm{I}}t$ then: update ${}_{\mathrm{I}}t = {}_{\mathrm{I}}t + {}_{\mathrm{I}}\Delta t$ and evaluate vectors ${}_{\mathrm{I}}\mathbf{L}^{t}$ and ${}_{\mathrm{I}}\mathbf{S}^{t}$
  (2.2) Iterative loop
    (2.2.1) Solve BE formulation III: obtain ${}^{(k+\alpha)}_{\mathrm{III}}\ddot{\mathbf{U}}^{\mathrm{III}t}$
    (2.2.2) Adoption of relaxation parameter: ${}^{(k+1)}_{\mathrm{III}}\ddot{\mathbf{U}}^{\mathrm{III}t} = (\alpha){}^{(k+\alpha)}_{\mathrm{III}}\ddot{\mathbf{U}}^{\mathrm{III}t} + (1-\alpha){}^{(k)}_{\mathrm{III}}\ddot{\mathbf{U}}^{\mathrm{III}t}$
    (2.2.3) From ${}^{(k+1)}_{\mathrm{III}}\ddot{\mathbf{U}}^{\mathrm{III}t}_{\mathrm{N}}$ obtain ${}^{(k+1)}_{\mathrm{I}}\ddot{\mathbf{U}}^{\mathrm{III}t}$ (Eq. (13c)/space interpolation – Fig. 2)
    (2.2.4) From ${}^{(k+1)}_{\mathrm{I}}\ddot{\mathbf{U}}^{\mathrm{III}t}$ obtain ${}^{(k+1)}_{\mathrm{I}}\ddot{\mathbf{U}}^{\mathrm{I}t}$ (time extrapolation – Fig. 1(a))
    (2.2.5) Solve BE formulation I: obtain ${}^{(k+1)}_{\mathrm{I}}\mathbf{P}^{\mathrm{I}t}$
    (2.2.6) From ${}^{(k+1)}_{\mathrm{I}}\mathbf{P}^{\mathrm{I}t}$ obtain ${}^{(k+1)}_{\mathrm{I}}\mathbf{P}^{\mathrm{III}t}$ (time interpolation – Fig. 1(b))
    (2.2.7) From ${}^{(k+1)}_{\mathrm{I}}\mathbf{P}^{\mathrm{III}t}$ obtain ${}^{(k+1)}_{\mathrm{III}}\mathbf{T}^{\mathrm{III}t}$ (Eqs. (13a) and (13b)/space interpolation – Fig. 2)
    (2.2.8) Check for convergence
  (2.3) Updating (and printing) of BE formulation III results
    If ${}_{\mathrm{III}}t + {}_{\mathrm{III}}\Delta t > {}_{\mathrm{I}}t$ then: updating (and printing) of BE formulation I results
  (2.4) Go to the next time step until the analysis is finished

(3) End of calculation

$$ {}_{\mathrm{I}}\mathbf{U}^{t} = {}_{\mathrm{I}}\mathbf{U}^{t_0} + {}_{\mathrm{I}}\dot{\mathbf{U}}^{t_0}(t-t_0) + {}_{\mathrm{I}}\ddot{\mathbf{U}}^{t}(t-t_0)^2/2 \quad \forall t \in (t_0; t_0 + {}_{\mathrm{I}}\Delta t] \tag{14} $$

where ${}_{\mathrm{I}}\Delta t$ is the time-step of the BE formulation I. According to Eq. (14), along each time-step ${}_{\mathrm{I}}\Delta t$, the equivalent displacements, velocities and accelerations (BE formulation I) have parabolic, linear and piecewise constant behavior, respectively (Fig. 1(a)). Eq. (14) is equivalent to the Newmark method [36], adopting the parameters: $\gamma = 1.00$ and $\beta = 0.50$. Eq. (14) has also been applied to some BEM–FEM coupling algorithms [37], giving good results.

Finally, a relation between ${}_{\mathrm{II}}\mathbf{U}^{t}$ and ${}_{\mathrm{I}}\mathbf{Q}^{t}$ can be numerically established as follows: analogously to Eq. (13c), ${}_{\mathrm{I}}\mathbf{U}^{t}$ can be related to ${}_{\mathrm{II}}\mathbf{U}^{t}_{\mathrm{N}}$ and, in the sequence, ${}_{\mathrm{I}}\mathbf{Q}^{t}$ can be related to ${}_{\mathrm{I}}\mathbf{U}^{t}$ by taking into account Eq. (14) (calculus of ${}_{\mathrm{I}}\ddot{\mathbf{U}}^{t}$) and relation ${}_{\mathrm{I}}\ddot{\mathbf{U}}^{t} = (1/\rho){}_{\mathrm{I}}\mathbf{Q}^{t}$.

In the iterative coupling of formulations I and II, natural boundary conditions are prescribed, at the common interfaces, for each sub-domain (either modeled by the BE formulation I or II). The displacements evaluated at the sub-domains modeled by formulation II are used to obtain the fluxes (prescribed interface boundary condition) for the sub-domains modeled by formulation I (see discussion above); the pressures evaluated at the sub-domains modeled by formulation I are used to obtain the tractions (prescribed interface boundary condition) for the sub-domains modeled by formulation II (analogously to Eqs. (13a) and (13b)). Concisely, each sub-domain is solved separately (${}_{\mathrm{II}}\mathbf{U}^{t}$ and ${}_{\mathrm{I}}\mathbf{P}^{t}$ are evaluated at each iterative step) and the interface relations ${}_{\mathrm{II}}\mathbf{U}^{t} \rightarrow {}_{\mathrm{I}}\mathbf{Q}^{t}$ and ${}_{\mathrm{I}}\mathbf{P}^{t} \rightarrow {}_{\mathrm{II}}\mathbf{T}^{t}$ are iteratively considered until convergence is achieved. A basic algorithm solution for the coupling of BE formulations I and II is shown in Table 2.

3.4. Coupling of formulations II and III

Taking into account a solid–solid interaction problem, the boundary conditions (equilibrium and continuity conditions, respectively) at coupling interfaces are given by:

Table 2
Iterative coupling of BE formulations I and II

(1) Initial calculations
  (1.1) Time steps for each sub-domain are selected (${}_{\mathrm{I}}\Delta t, {}_{\mathrm{II}}\Delta t$)
    The following initial time attribution is adopted: ${}_{\mathrm{I}}t = {}_{\mathrm{I}}\Delta t$; ${}_{\mathrm{II}}t = 0$
  (1.2) BEM standard initial calculations are considered (e.g. influence matrices $\mathbf{G}^1$, $\mathbf{H}^1$, etc.)
  (1.3) Initial prescribed values are chosen at the common interface surfaces (e.g. ${}_{\mathrm{II}}{}^{(0)}\mathbf{T} = \mathbf{0}$)
(2) Time-step loop
  (2.1) Beginning of evaluations at each time step
    Update ${}_{\mathrm{II}}t = {}_{\mathrm{II}}t + {}_{\mathrm{II}}\Delta t$ and evaluate vectors ${}_{\mathrm{II}}\mathbf{L}^{{}_{\mathrm{II}}t}$ and ${}_{\mathrm{II}}\mathbf{S}^{{}_{\mathrm{II}}t}$
    If ${}_{\mathrm{II}}t > {}_{\mathrm{I}}t$ then: update ${}_{\mathrm{I}}t = {}_{\mathrm{I}}t + {}_{\mathrm{I}}\Delta t$ and evaluate vectors ${}_{\mathrm{I}}\mathbf{L}^{{}_{\mathrm{I}}t}$ and ${}_{\mathrm{I}}\mathbf{S}^{{}_{\mathrm{I}}t}$
  (2.2) Iterative loop
    (2.2.1) Solve BE formulation II: obtain ${}_{\mathrm{II}}^{(k+\alpha)}\mathbf{U}^{\mathrm{II}^t}$
    (2.2.2) Adoption of relaxation parameter: ${}_{\mathrm{II}}^{(k+1)}\mathbf{U}^{\mathrm{II}^t} = (\alpha){}_{\mathrm{II}}^{(k+\alpha)}\mathbf{U}^{\mathrm{II}^t} + (1-\alpha){}_{\mathrm{II}}^{(k)}\mathbf{U}^{\mathrm{II}^t}$
    (2.2.3) From ${}_{\mathrm{II}}^{(k+1)}\mathbf{U}_{\mathrm{N}}^{\mathrm{II}^t}$ obtain ${}_{\mathrm{I}}^{(k+1)}\mathbf{U}^{\mathrm{II}^t}$ (space interpolation – Fig. 2)
    (2.2.4) From ${}_{\mathrm{I}}^{(k+1)}\mathbf{U}^{\mathrm{II}^t}$ obtain ${}_{\mathrm{I}}^{(k+1)}\ddot{\mathbf{U}}^{\mathrm{II}^t}$ (Eq. (14)):
      ${}_{\mathrm{I}}^{(k+1)}\ddot{\mathbf{U}}^{\mathrm{II}^t} = (2/\Delta\hat{t}^2)({}_{\mathrm{I}}^{(k+1)}\mathbf{U}^{\mathrm{II}^t} - {}_{\mathrm{I}}\mathbf{U}^{{}_{\mathrm{I}}t-{}_{\mathrm{I}}\Delta t}) - (2/\Delta\hat{t})({}_{\mathrm{I}}\dot{\mathbf{U}}^{{}_{\mathrm{I}}t-{}_{\mathrm{I}}\Delta t})$
    (2.2.5) From ${}_{\mathrm{I}}^{(k+1)}\ddot{\mathbf{U}}^{\mathrm{II}^t}$ obtain ${}_{\mathrm{I}}^{(k+1)}\ddot{\mathbf{U}}^{\mathrm{I}^t}$ (time extrapolation – Fig. 1(a))
    (2.2.6) Solve BE formulation I: obtain ${}_{\mathrm{I}}^{(k+1)}\mathbf{P}^{\mathrm{I}^t}$
    (2.2.7) From ${}_{\mathrm{I}}^{(k+1)}\mathbf{P}^{\mathrm{I}^t}$ obtain ${}_{\mathrm{I}}^{(k+1)}\mathbf{P}^{\mathrm{II}^t}$ (time interpolation – Fig. 1(b))
    (2.2.8) From ${}_{\mathrm{I}}^{(k+1)}\mathbf{P}^{\mathrm{II}^t}$ obtain ${}_{\mathrm{II}}^{(k+1)}\mathbf{T}^{\mathrm{II}^t}$ (Eqs. (13a) and (13b)/space interpolation – Fig. 2)
    (2.2.9) Check for convergence
  (2.3) Updating (and printing) of BE formulation II results
    If ${}_{\mathrm{II}}t + {}_{\mathrm{II}}\Delta t > {}_{\mathrm{I}}t$ then: updating (and printing) of BE formulation I results (including ${}_{\mathrm{I}}\mathbf{U}^{{}_{\mathrm{I}}t} = {}_{\mathrm{I}}\mathbf{U}^{{}_{\mathrm{I}}t-{}_{\mathrm{I}}\Delta t} + ({}_{\mathrm{I}}\Delta t){}_{\mathrm{I}}\dot{\mathbf{U}}^{{}_{\mathrm{I}}t-{}_{\mathrm{I}}\Delta t} + ({}_{\mathrm{I}}\Delta t^2/2){}_{\mathrm{I}}\ddot{\mathbf{U}}^{{}_{\mathrm{I}}t}$ and ${}_{\mathrm{I}}\dot{\mathbf{U}}^{{}_{\mathrm{I}}t} = {}_{\mathrm{I}}\dot{\mathbf{U}}^{{}_{\mathrm{I}}t-{}_{\mathrm{I}}\Delta t} + ({}_{\mathrm{I}}\Delta t){}_{\mathrm{I}}\ddot{\mathbf{U}}^{{}_{\mathrm{I}}t}$)
  (2.4) Go to the next time step until the analysis is finished
(3) End of calculation

$$ {}_{\mathrm{III}}\mathbf{T}^t + {}_{\mathrm{II}}\mathbf{T}^t = \mathbf{0} \tag{15a} $$

$$ {}_{\mathrm{III}}\mathbf{U}^t - {}_{\mathrm{II}}\mathbf{U}^t = \mathbf{0} \tag{15b} $$

where Eq. (15) is written based on the coupling of BE formulations II and III for a given time value t (thus the left-side subscripts II and III and the right-side superscript t).

In the iterative coupling of formulations II and III, at the common interfaces, natural boundary conditions are prescribed for the sub-domains modeled by the BE formulation III and essential boundary conditions are prescribed for the sub-domains modeled by the BE formulation II. The displacements evaluated at the sub-domains modeled by formulation III are used to obtain the interface displacements (prescribed interface

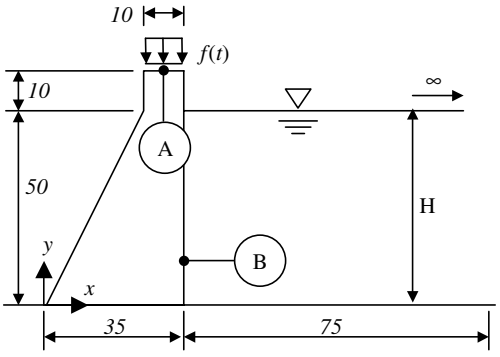

Fig. 3. Sketch of the dam-reservoir system: fluid–structure interaction problem (point A: $x = 30$ m, $y = 60$ m; point B: $x = 35$ m, $y = 10$ m).

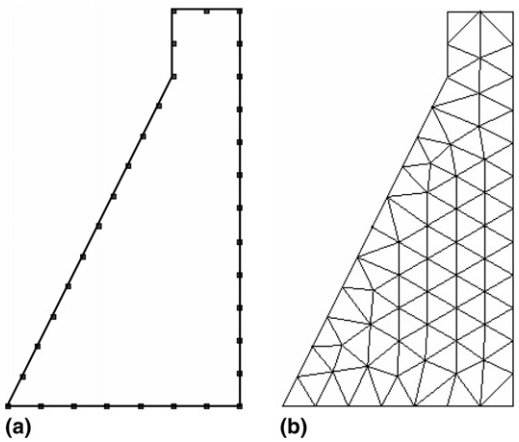

Fig. 4. BEM meshes for the dam: (a) boundary discretization – 34 linear boundary elements (BE formulations II and III); (b) domain discretization – 102 linear triangular cells (BE formulation III).

boundary condition) for the sub-domains modeled by formulation II (Eq. (15b)); the tractions evaluated at the sub-domains modeled by formulation II are used to obtain the tractions (prescribed interface boundary condition) for the sub-domains modeled by formulation III (Eq. (15a)). Concisely, each sub-domain is solved separately (${}_{III}\mathbf{U}^t$ and ${}_{II}\mathbf{T}^t$ are evaluated at each iterative step) and the interface relations ${}_{III}\mathbf{U}^t \rightarrow {}_{II}\mathbf{U}^t$ and

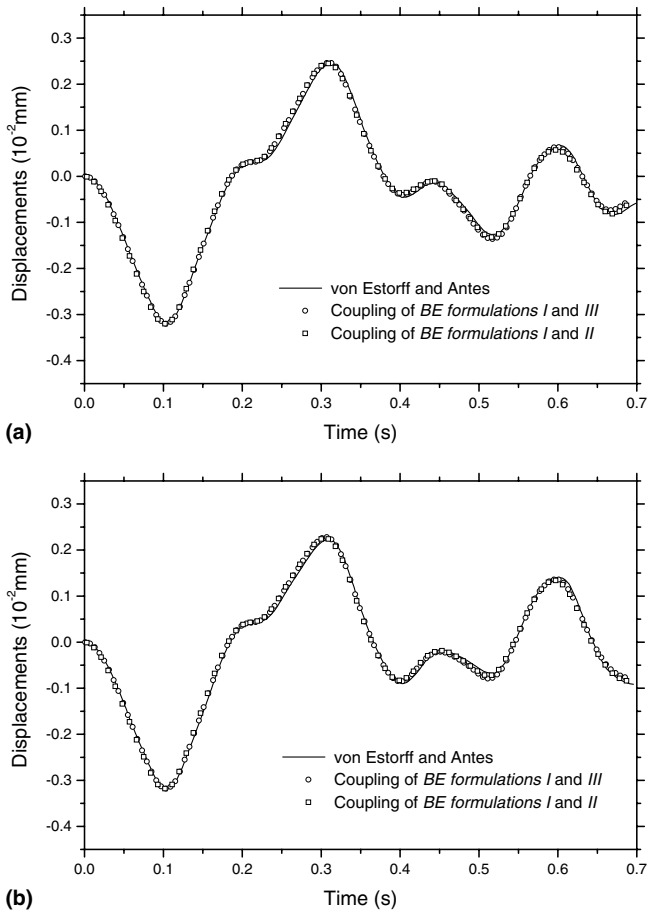

Fig. 5. Vertical displacements at point A: (a) $H = 35$ m; (b) $H = 50$ m.

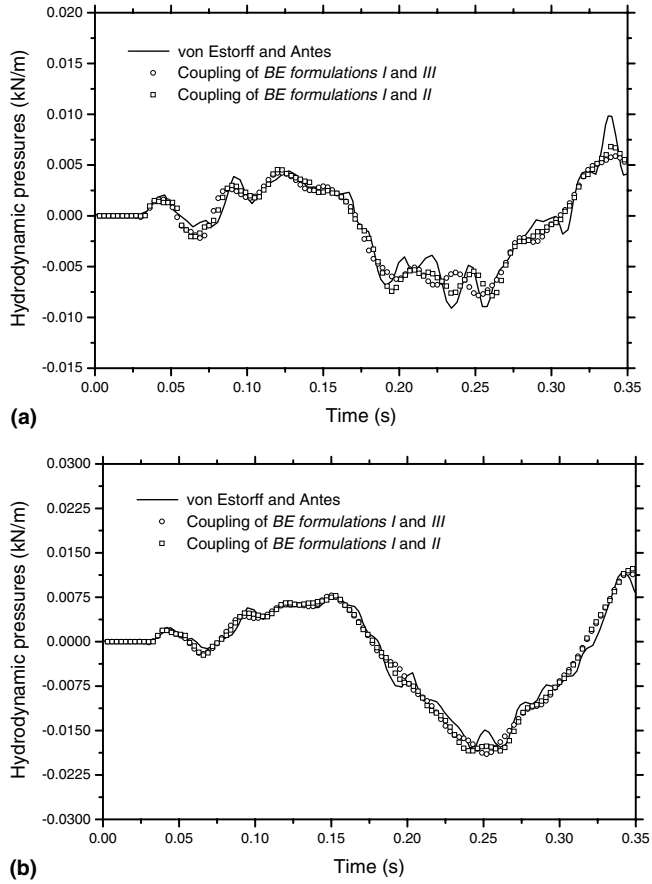

Fig. 6. Hydrodynamic pressures at point B: (a) $H = 35$ m; (b) $H = 50$ m.

${}_{\mathrm{II}}\mathbf{T}^t \rightarrow {}_{\mathrm{III}}\mathbf{T}^t$ are iteratively considered until convergence is achieved. The iterative coupling of formulations II and III is described in detail in [27].

4. Numerical applications

Two numerical examples are considered here. The first one deals with a loaded dam retaining the water of a storage-lake (fluid–structure interaction problem). The second one is concerned with the analysis of a channel

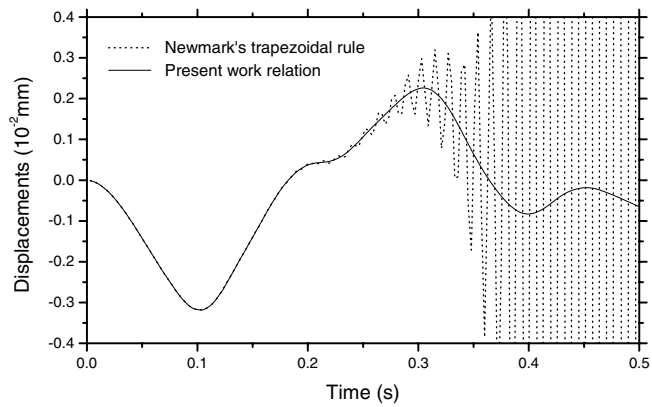

Fig. 7. Vertical displacements at point A considering different interface relations (${}_{\mathrm{II}}\mathbf{U}^t \rightarrow {}_{\mathrm{I}}\mathbf{Q}^t$) for the coupling of BE formulations I and II.

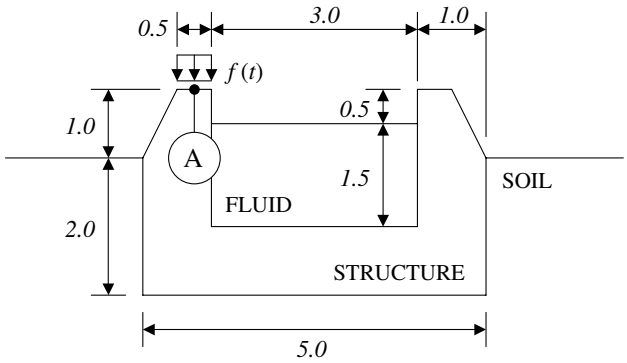

Fig. 8. Sketch of the channel system: fluid–soil–structure interaction problem.

(fluid–soil–structure interaction problem). For some examples concerning solid–solid interaction problems, the authors' previous work [27] is indicated. For all examples presented here, a relaxation parameter $\alpha = 0.5$ was adopted.

4.1. Example I

In this first example, a dam-reservoir system, as depicted in Fig. 3, is analyzed [14]. The structure is subjected to a sinusoidal distributed vertical load on its crest, acting with an angular frequency $w = 18$ rad/s. The material properties of the dam are: Poisson's ratio $v = 0.25$; Young's modulus $E = 3.437 \times 10^6$ N/m^2; mass density $\rho = 2000$ kg/m^3. The adjacent fluid is characterized by a mass density $\rho = 1000$ kg/m^3 and a wave velocity $c = 1436$ m/s.

The dam-reservoir system is solved here taking into account the coupling of BE formulations I and II, as well as the coupling of BE formulations I and III. The BEM meshes adopted to model the dam are depicted in Fig. 4: 34 linear boundary elements of equal length (BE formulations II and III) and 102 linear triangular cells

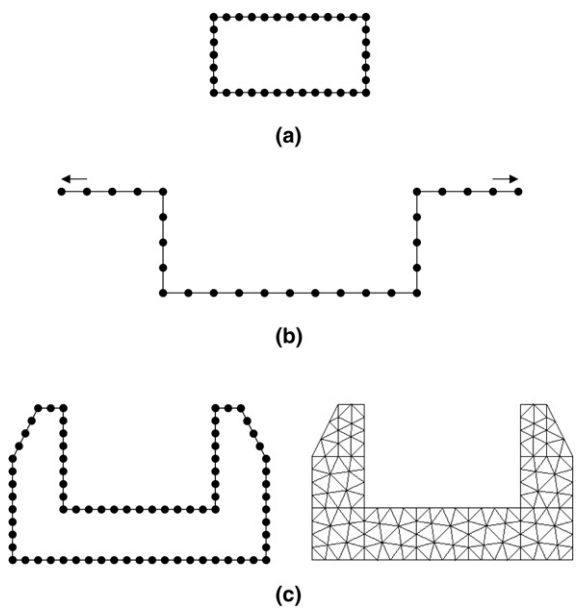

Fig. 9. BEM meshes: (a) BE formulation I – 36 linear boundary elements; (b) BE formulation II – 118 linear boundary elements; (c) BE formulation III – 74 linear boundary elements and 196 linear triangular cells.

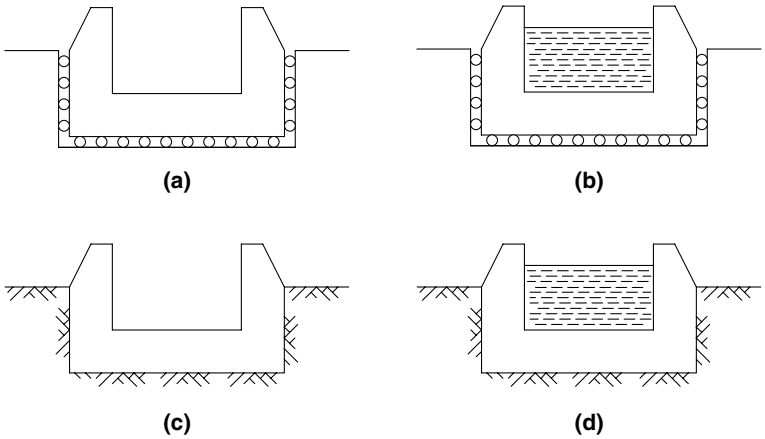

Fig. 10. Channel system modeling: (a) model 1 (structure); (b) model 2 (fluid–structure); (c) model 3 (soil–structure); (d) model 4 (fluid–soil–structure).

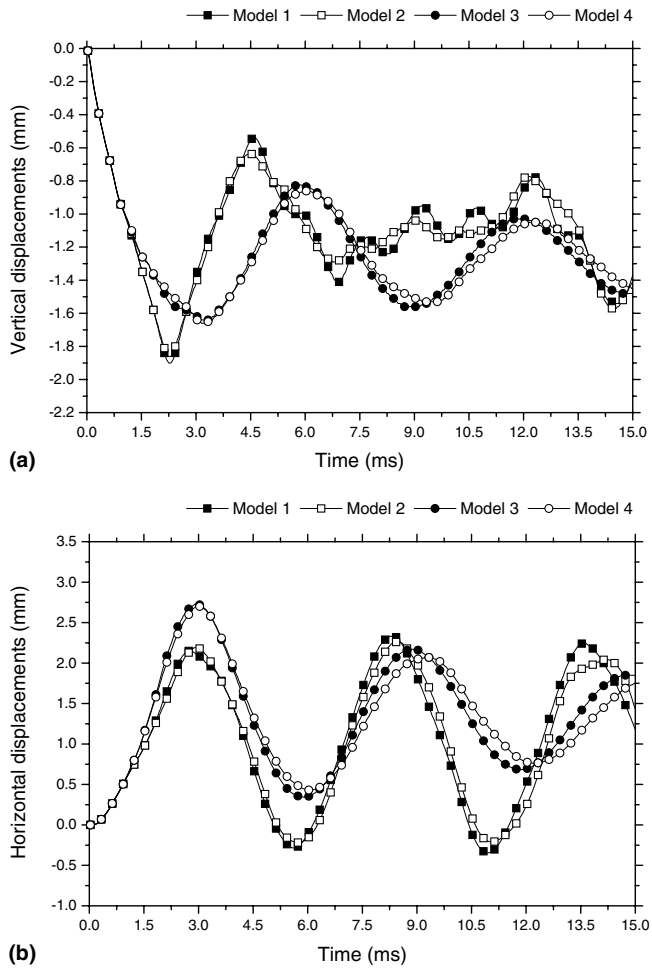

Fig. 11. Displacements at point A for models 1, 2, 3 and 4: elastic analysis.

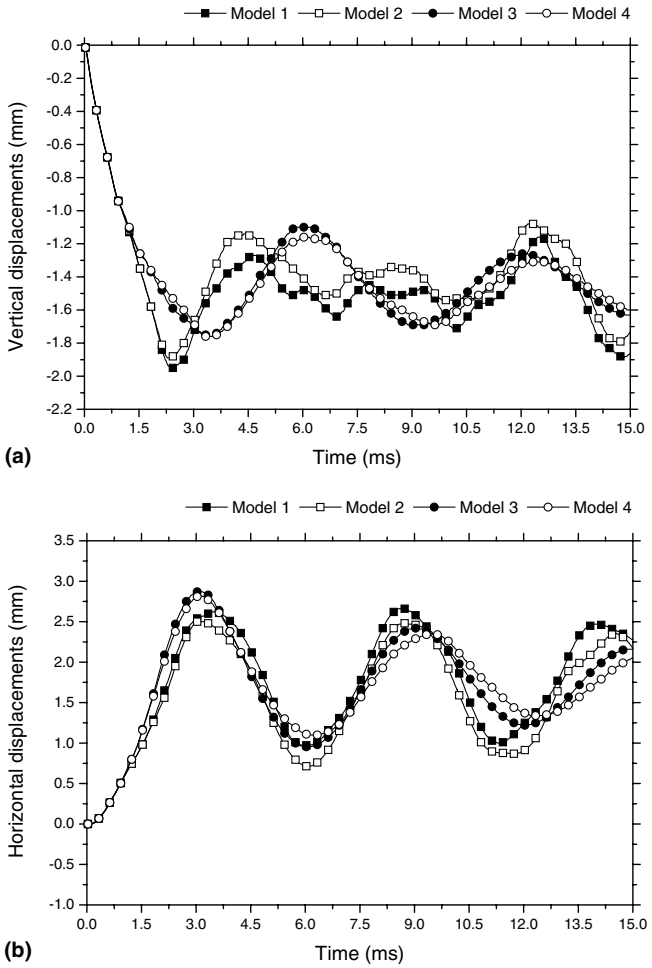

Fig. 12. Displacements at point A for models 1, 2, 3 and 4: elastoplastic analysis.

(BE formulation III) are employed. To model the fluid, acoustic boundary elements of constant length $\ell = 5$ m (BE formulation I) have been adopted (the number of elements depends on the water level H). Different time-steps were considered for each sub-domain (in order to obtain an optimal modeling within each sub-domain), they are: ${}_{\mathrm{I}}\Delta t = 0.003$ s; ${}_{\mathrm{II}}\Delta t = 0.003$ s and ${}_{\mathrm{III}}\Delta t = 0.001$ s.

In Fig. 5, vertical displacements time history at point A is depicted, taking into account two different water levels: $H = 50$ m and $H = 35$ m. In Fig. 6, the hydrodynamic pressures at point B are shown. As one can observe, the results considering the coupling of BE formulation I and II and the coupling of BE formulation I and III are in good agreement between each other, as well as with the results previously presented by von Estorff and Antes [14].

In Fig. 7, vertical displacements at point A are depicted ($H = 50$ m) considering different interface relations (${}_{\mathrm{II}}\mathbf{U}^t \rightarrow {}_{\mathrm{I}}\mathbf{Q}^t$) for the coupling of BE formulations I and II. As it has been discussed, the present work adopts Eq. (14) to relate ${}_{\mathrm{II}}\mathbf{U}^t$ and ${}_{\mathrm{I}}\mathbf{Q}^t$. Eq. (14) is consistent with the BE formulations in use. Once one takes into account other non-consistent relations to relate ${}_{\mathrm{II}}\mathbf{U}^t$ and ${}_{\mathrm{I}}\mathbf{Q}^t$ (e.g. Newmark's Trapezoidal rule – see Fig. 7, the Houbolt method, etc.), instabilities may occur.

4.2. Example II

In this example, a fluid–soil–structure interaction problem is analyzed [21]. A sketch of the model is depicted in Fig. 8. The material properties are: (i) fluid: mass density $\rho = 1000$ kg/m^3; wave velocity

$c = 1436$ m/s; (ii) soil: Poisson's ratio $v = 0.3$; Young's modulus $E = 2.66 \times 10^7$ kN/m^2; mass density $\rho = 2700$ kg/m^3; (iii) structure: Poisson's ratio $v = 0.25$; Young's modulus $E = 8.87 \times 10^6$ kN/m^2; mass density $\rho = 1500$ kg/m^3. A perfectly plastic material obeying the von Mises yield criterion is assumed for the structure with uniaxial yield stress $\sigma_0 = 6.0 \times 10^3$ kN/m^2.

The BEM meshes adopted to model each sub-domain are presented in Fig. 9. The time steps adopted are, at each sub-domain: ${}_{\mathrm{I}}\Delta t = 12 \times 10^{-5}$ s ($\beta \approx 0.69$); ${}_{\mathrm{II}}\Delta t = 12 \times 10^{-5}$ s ($\beta \approx 0.87$) and ${}_{\mathrm{III}}\Delta t = 3 \times 10^{-5}$ s ($\beta \approx 0.32$), where $\beta = c\Delta t/\ell$. Four different models, taking into account different interaction levels, are employed to solve the problem, as depicted in Fig. 10. Displacements at point A are depicted in Figs. 11 and 12, taking into account elastic and elastoplastic models, respectively. As one can notice, significant difference may be observed according to the different levels of interaction adopted.

5. Conclusions

The present paper presented iterative BEM–BEM coupling procedures to model time-domain wave propagation through different interacting physical sub-regions. The following BEM formulations were considered here: (i) formulation I: acoustic time-domain formulation based on time-dependent Green's functions; (ii) formulation II: elastodynamic time-domain formulation based on time-dependent Green's functions; (iii) formulation III: dynamic time-domain formulation based on static Green's functions, employed here to model regions with elastoplastic behavior. Formulations I and II are quite suitable for infinite domain cases and for bounded domain linear analyses, whereas formulation III is ideal when one wishes to deal with non-linear behavior (elastoplastic analysis in the present case) by a BEM approach.

A new procedure for coupling time-domain acoustic and elastic (or elastoplastic) BEM algorithms has been introduced. The examples analyzed showed that the proposed procedure leads to stable and accurate results for both cases studied: coupling of formulations I and II, and coupling of formulations I and III. Good results concerning the coupling of formulations II and III were also once more presented.

The iterative coupling procedure presented converges in few iterations (see Ref. [27]), thus, it is more economical than direct coupling approaches. As shown here, iterative coupling approaches bears another important advantage over direct coupling: different time steps and mesh refinement are allowed for each sub-domain; thus, it is possible to achieve stability in cases where direct coupling algorithms lead to unstable results.

References

[1] O.C. Zienkiewicz, R.L. TaylorThe Finite Element Method, fifth ed., vols. 1–3, Butterworth-Heinemann, Oxford, 2002 (reprinted).
[2] T.J.R. Hughes, The Finite Element Method – Linear Static and Dynamic Finite Element Analysis, Dover Publications, Mineola, New York, 2000.
[3] W.J.T. Daniel, Analysis and implementation of a new constant acceleration subcycling algorithm, International Journal for Numerical Methods in Engineering 40 (1997) 2841–2855.
[4] P. Smolinski, Subcycling integration with non-integer time steps for structural dynamics problems, Computers & Structures 59 (1996) 273–281.
[5] T. Belytschko, Y.Y. Lu, Explicit multi-time step integration for first and second order finite element semi-discretization, Computer Methods in Applied Mechanics and Engineering 108 (1993) 353–383.
[6] J. Virieux, P-SV wave propagation in heterogeneous media: velocity–stress finite difference method, Geophysics 51 (1986) 889–901.
[7] G. Cohen, P. Joly, Fourth order schemes for the heterogeneous acoustics equation, Computer Methods in Applied Mechanics and Engineering 80 (1990) 397–407.
[8] B. Lombard, J. Piraux, Numerical treatment of two-dimensional interfaces for acoustic and elastic waves, Journal of Computational Physics 195 (2004) 90–116.
[9] C.A. Brebbia, The Boundary Element Method for Engineers, Pentech Press, London, 1978.
[10] O.C. Zienkiewicz, D.M. Kelly, P. Bettess, The coupling of the finite element method and boundary solution procedures, International Journal for Numerical Methods in Engineering 11 (1977) 355–376.
[11] C.A. Brebbia, P. Georgiou, Combination of boundary and finite elements in elastostatics, Applied Mathematical Modelling 3 (1979) 212–220.
[12] D.L. Karabalis, D.E. Beskos, Dynamic response of 3-D flexible foundations by time domain BEM and FEM, Soil Dynamics and Earthquake Engineering 4 (1985) 91–101.

[13] O. von Estorff, M.J. Prabucki, Dynamic response in time domain by coupled boundary and finite elements, Computational Mechanics 6 (1990) 35–46.
[14] O. von Estorff, H. Antes, On FEM–BEM coupling for fluid–structure interaction analysis in the time domain, International Journal for Numerical Methods in Engineering 31 (1991) 1151–1168.
[15] O. von Estorff, Coupling of BEM and FEM in the time domain: some remarks on its applicability and efficiency, Computers & Structures 44 (1992) 325–337.
[16] T. Belytschko, Y.Y. Lu, A variational coupled FE–BE method for transient problems, International Journal for Numerical Methods in Engineering 37 (1994) 91–105.
[17] O. von Estorff, M. Firuziaan, Coupled BEM/FEM approach for nonlinear soil/structure interaction, Engineering Analysis with Boundary Elements 24 (2000) 715–725.
[18] O. Czygan, O. von Estorff, Fluid–structure interaction by coupling BEM and nonlinear FEM, Engineering Analysis with Boundary Elements 26 (2002) 773–779.
[19] G. Yu, W.J. Mansur, J.A.M. Carrer, S.T. Lie, A more stable scheme for BEM/FEM coupling applied to two-dimensional elastodynamics, Computers & Structures 79 (2001) 811–823.
[20] G.Y. Yu, S.T. Lie, S.C. Fan, Stable boundary element method/finite element method procedure for dynamic fluid structure interactions, Journal of Engineering Mechanics 128 (2002) 909–915.
[21] D. Soares Jr., Dynamic analysis of non-linear soil–fluid–structure coupled systems by the finite element method and the boundary element method (in Portuguese), Ph.D. Thesis. Federal University of Rio de Janeiro, Brazil, 2004.
[22] W.M. Elleithy, H.J. Al-Gahtani, An overlapping domain decomposition approach for coupling the finite and boundary element methods, Engineering Analysis with Boundary Elements 24 (2000) 391–398.
[23] W.M. Elleithy, H.J. Al-Gahtani, M. El-Gebeily, Iterative coupling of BE and FE methods in elastostatics, Engineering Analysis with Boundary Elements 25 (2001) 685–695.
[24] D. Soares Jr., O. von Estorff, Combination of FEM and BEM by an iterative coupling procedure, in: 4th European Congress on Computational Methods in Applied Sciences and Engineering, ECCOMAS 2004, Jyväskylä, Finland, 2004.
[25] D. Soares Jr., O. von Estorff, W.J. Mansur, Iterative coupling of BEM and FEM for nonlinear dynamic analyses, Computational Mechanics 34 (2004) 67–73.
[26] D. Soares Jr., O. von Estorff, W.J. Mansur, Efficient nonlinear solid–fluid interaction analysis by an iterative BEM/FEM coupling, International Journal for Numerical Methods in Engineering 64 (2005) 1416–1431.
[27] D. Soares Jr., J.A.M. Carrer, W.J. Mansur, Non-linear elastodynamic analysis by the BEM: an approach based on the iterative coupling of the D-BEM and TD-BEM formulations, Engineering Analysis with Boundary Elements 29 (2005) 761–774.
[28] W.J. Mansur, A time-stepping technique to solve wave propagation problems using the boundary element method, Ph.D. Thesis, University of Southampton, England, 1983.
[29] J.A.M. Carrer, J.C.F. Telles, A boundary element formulation to solve transient dynamic elastoplastic problems, Computers & Structures 13 (1992) 707–713.
[30] J. Dominguez, Boundary Elements in Dynamics, Computational Mechanics Publications, Southampton, Boston, 1993.
[31] J.A.M. Carrer, W.J. Mansur, Time-domain BEM analysis for the 2D scalar wave equation: initial conditions contributions to space and time derivatives, International Journal for Numerical Methods in Engineering 39 (1996) 2169–2188.
[32] J.A.M. Carrer, Implicit techniques to solve static and transient dynamic elastoplastic problems by the boundary element method (in Portuguese), Ph.D. Thesis, Federal University of Rio de Janeiro, Brazil, 1991.
[33] J.C.F. Telles, The Boundary Element Method Applied to Inelastic Problems, Springer-Verlag, Berlin, 1983.
[34] J.C. Houbolt, A recurrence matrix solution for the dynamic response of elastic aircraft, Journal of the Aeronautical Sciences 17 (1950) 540–550.
[35] J.A.M. Carrer, J.C.F. Telles, Static and dynamic nonlinear stress analysis, in: G.D. Manolis, T.G. Davies (Eds.), Boundary Element Techniques in Geomechanics, Elsevier Applied Science, London, 1993.
[36] N.M. Newmark, A method of computation for structural dynamics, ASCE Journal of Engineering Mechanics Division 85 (1959) 67–94.
[37] D. Soares Jr., W.J. Mansur, An efficient time-domain BEM/FEM coupling for acoustic–elastodynamic interaction problems, CMES: Computer Modeling in Engineering Sciences 8 (2005) 153–164.